Technical University of Denmark

Experimental and theoretical demonstration of amplifying pulse compression using an SOA- based Mach-Zehnder Interferometer

Nielsen, Mads Lønstrup; Dagens, B.

Published in:
Proc. of LEOS Annual Meeting 2004

Link to article, DOI:
10.1109/LEOS.2004.1363420

Publication date:
2004

Document Version
Publisher's PDF, also known as Version of record

Experimental and theoretical demonstration of amplifying pulse compression using an SOA-based Mach-Zehnder Interferometer

Mads L. Nielsen[1] and Beatrice Dagens[2]

[1]COM, Technical University of Denmark, Building 345V, DK-2800 Kgs. Lyngby, Denmark (mln@com.dtu.dk),
[2]Alcatel-Thales III-V lab, Route de Nozay, 91460 Marcoussis, France

Introduction

Schemes for compressing optical pulses have received considerable attention over the last two decades, due to the need for dispersion compensation in optical communication systems, and an increasing interest for ultra-short pulses for optical sampling and for high-speed optical time-division multiplexed (OTDM) systems [1]. In its simplest form, pulse compression is obtained by exploiting that fiber group velocity dispersion (GVD) introduces a linear chirp across the pulse, which is able to compensate for pulse broadening caused by a linear chirp of opposite sign. This is the principle of the dispersion compensating fiber. However, if the pulse to be compressed is transform-limited, or has acquired a chirp that is nonlinear, this technique cannot be applied. In this case a pulse compressor based on e.g. a combination of GVD and self-phase modulation (SPM) is required [2]. Such nonlinear fiber based approaches are very powerful, but lack the potential for integration with optoelectronic components such as lasers and modulators. In this paper we propose a pulse compression scheme based on a Semiconductor Optical Amplifier (SOA)-based Mach-Zehnder interferometer (MZI). It is independent of the initial chirp of the pulses, provides amplification, and can potentially be integrated with a simple pulse source, such as a gain-switched DFB (GS-DFB) laser. The scheme is demonstrated experimentally, and simulations provide further insight.

Principle and modeling

The compression scheme is illustrated in Fig. 1: a pulse train is launched into port 1 of the MZI, and appears at port 2 with a reduced pulse width. To assist in explaining the pulse compression, a numerical analysis, based on a detailed time-domain model of the SOA-based MZI, has been carried out.

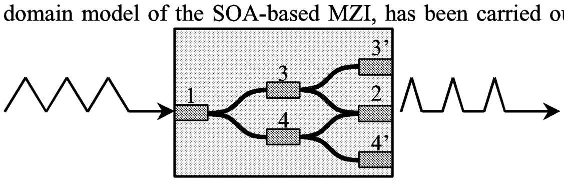

Fig. 1: *Sketch of SOA-MZI based pulse compressor*

The input to the numerical model is a 10 GHz pulse train consisting of 25 ps wide (FWHM) Gaussian pulses with an average power of +2 dBm. SOAs 3 and 4 are 1.2 mm long, with a cross section of 1.2x0.2 μm and a corresponding confinement factor of 0.4, whereas the remaining SOAs are assumed passive. Fig. 2 (left axis) shows the pulse shape at port 2 for the cases where only SOA 3 is on (solid), only SOA 4 is on (thin dashed), and both SOAs are on (thick dashed). Focusing on the scenarios where only one SOA is on, the pulse shape is observed to be highly asymmetric. This is because the pulse saturates the carrier population, and consequently the gain, on the leading edge, leaving less gain for the center and trailing edge of the pulse. The current supplied to SOAs 3 and 4 are 340 mA and 150 mA, respectively, and thus the available gain is higher for SOA 3. The saturation energy is reached earlier in the pulse for a higher gain, which is reflected by a larger shift of the pulse peak towards the leading edge.

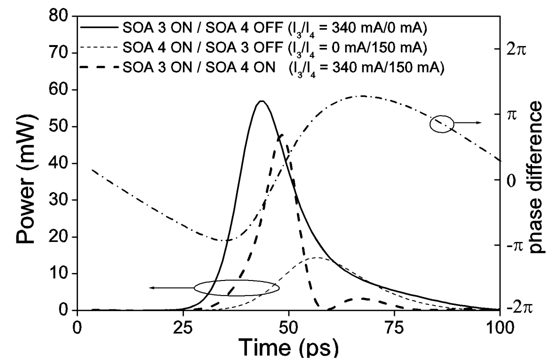

Fig. 2: *Output pulse shapes for only SOA 4 on, only SOA 3 on, and both SOAs on for I_3/I_4 = 340/150 mA. Phase difference on right axis.*

The carrier modulation in the two SOAs also leads to SPM [3], and due to the different bias currents, the phase modulation in the two arms is highly asymmetric. The phase difference between the two interferometer arms is shown on the right axis of Fig. 2. At the leading edge of the pulse in SOA 3 the phase difference is -π, corresponding to destructive interference, then it increases to 0 (constructive interference) between the peaks of the individual pulses, and finally attains a value of around π at trailing edge, where the pulses from the two arms coincide. This destructive interference efficiently suppresses the long trailing edge, and leads to a reduction of the pulse width. It should be noticed that the compressed pulse is trailed by a weak "satellite pulse", since the phase difference deviates slightly from π over the trailing edge of the pulses. In the present example the satellite pulse is suppressed by around 11 dB compared to the pulse peak, and with an optimization of operating conditions and device structure this suppression ratio is expected to increase. It is important to point out that the principle of pulse compression is independent of the chirp of the input pulses, since it relies only on carrier modulation. Moreover, the relative pulse width reduction is expected to be insensitive to the input pulse width τ_{in}, as long as $\tau_{cr}<\tau_{in}<<\tau_{sp}$, where τ_{cr} is the critical pulse width, below which the effect of interband carrier dynamics is significant (~ 2 ps), and τ_{sp} is the spontaneous carrier lifetime (~ 200 ps – 1 ns) [4].

In the scenario illustrated in Fig. 2, the current through SOA 3, I_3, has been optimized to provide a minimum pulse width for I_4 = 150 mA. The pulse width (FWHM) vs. I_3 is shown in Fig. 3, where the oscillations are an artifact of the interferometric nature of the pulse compressor. The minimum width of ~12 ps is obtained for I_3 = 340 mA.

0-7803-8557-8/04/$20.00©2004 IEEE

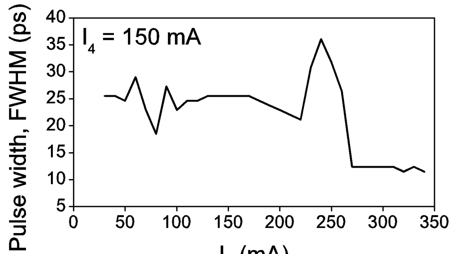

Fig 3: *Pulse width vs. I_3 for I_4 = 150 mA*

Experimental demonstration

The concept was demonstrated with an all-active MZI with the same SOA dimensions as used in the simulations. The input signal was generated by a GS-DFB, emitting a 10 GHz train of 25 ps wide pulses at 1556.5 nm. After amplification in an EDFA (to compensate for loss in polarization controller before the MZI + coupling loss), an average power of +5 dBm (measured in the fiber) was launched into port 1. Bias currents I_1 and I_2 were set to just above transparency to prevent a saturation-induced reduction of the extinction ratio at the input and output, and I_3'/I_4' were turned off. As in the simulation, I_3 was optimized for a fixed I_4, in this case I_4 = 180 mA. The result is shown in the trace in Fig. 4, measured in a 40 GHz bandwidth.

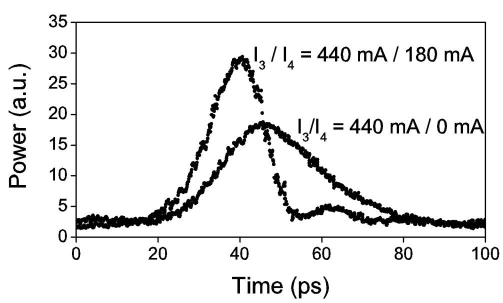

Fig. 4: *Output pulse shape for SOA 3 on and both SOAs on*

This result is in qualitative agreement with the modeling result in Fig. 3, except that the compressed pulse peaks before the pulse out of SOA 3. From Fig. 3 it is clear that this behavior occurs if the phase difference is ~0 on the leading edge, which may be caused by a phase offset in the interferometer. Notice that the prediction of a satellite pulse is correct. The width of the compressed pulse was estimated at 14.5 ps from an autocorrelation, assuming Gaussian pulse shape, which agrees reasonably well with the modeling. The average output power was +8 dBm (in the fiber), corresponding to a fiber-to-fiber gain of 3 dB.

It should be mentioned that a configuration similar to the one presented here has been proposed for compensating for saturation-induced patterning effects [5].

Transmission properties

Due to the carrier modulation imposed by the 10 GHz RF signal driving the GS-DFB, the leading edges and trailing edges of the pulses are blue-shifted and red-shifted, respectively. As a result the transmission properties are very poor, with a sensitivity degradation, compared to back-to-back, of 6.4 dB after only 4 km on standard single-mode fiber (SMF).

Suppressing the red-shifted edge by passing the clock signal through a narrow 0.3 nm wide (FWHM) band-pass filter (BPF), detuned 0.8 nm to the blue side, before modulating with 10 Gb/s data (PRBS 2^{31}-1), the transmission performance is improved dramatically. This is due to a reduction of the spectral width, and the results are illustrated in Fig. 5, which shows the eye diagram after 9 km on SMF without the filter (a), corresponding to an undetectable signal, and including the filter (b), corresponding to a 3 dB sensitivity degradation. The BPF reduces the pulse width from 25 ps to ~12 ps (right after the BPF) by suppressing the trailing edge. However, this compression is only possible because the pulses are heavily chirped.

The functionality of the filter may also be obtained using the MZI, since, according to Fig. 2, the MZI also suppresses the trailing edge. Fig. 5 (c) shows the eye diagram after 9 km of SMF, corresponding to a sensitivity degradation of ~2.5 dB.

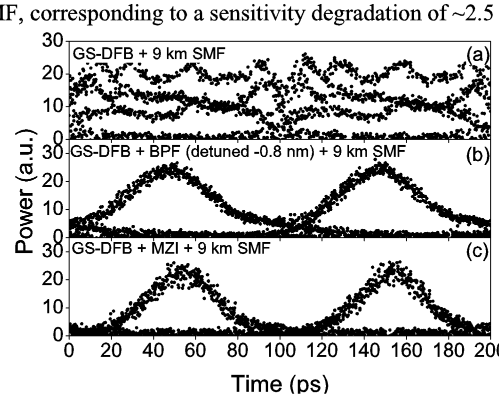

Fig. 5: *10 Gb/s eye diagrams after 9 km on SMF, (a) w/o BPF, (b) w/ BPF, (c) w/SOA-MZI*

In addition to improving the transmission performance of chirped pulse sources, filtering the output of an SOA has also been shown to compensate for saturation-induced patterning, thereby enhancing the input power dynamic range [6-7].

Conclusions

An amplifying SOA-MZI-based pulse compression scheme, independent of the initial chirp, has been proposed and demonstrated experimentally. Compression is obtained primarily by suppression of the trailing pulse edges, which was shown to significantly improve the transmission performance of a chirping GS-DFB, by suppressing the red-shift. The principle of pulse compression in a MZI was described through simulations, which illustrated good agreement with experimental results, with a compression of ~50%. An SOA-MZI can be integrated with e.g a GS-DFB or EAM to realize a source with tunable pulse width and superior transmission properties.

References

[1] R. J. Runser et al., Opt. and Quant. Electr. **33** (10), 2001
[2] G. P. Agrawal, Nonlinear Fiber Optics, 2. ed., Acad. Press
[3] G. P. Agrawal et al., J. Quant. Electron **25** (11), 1989
[4] A. Mecozzi et al., J. Opt. Soc. Am. B **14** (4), 1997
[5] Q. Xu et al., Photonics Technol. Lett. **13** (12), 2001
[6] J. Yu et al., J. Lightwave Technol. **19** (9), 2001
[7] C. S. Wong et al., Optics Comm. 232, 2004